Small Solitary Pulmonary Nodules (≤1 cm) Detected at Population-Based CT Screening for Lung Cancer: Reliable High-Resolution CT Features of Benign Lesions

Shodayu Takashima[1]
Shusuke Sone[2]
Feng Li[1]
Yuichiro Maruyama[1]
Minoru Hasegawa[1]
Tsuyoshi Matsushita[1]
Fumiyoshi Takayama[2]
Masumi Kadoya[1]

OBJECTIVE. We assessed thin-section CT features specific to benignity in solitary pulmonary nodules of 1 cm or smaller that were detected at population-based CT screening for lung cancer.

MATERIALS AND METHODS. Two reviewers independently made qualitative (presence or absence of lobulation, spiculation, air bronchogram, cavity, satellite lesions, pleural tag, concave margins, polygonal shape, and peripheral subpleural lesion) and quantitative (lesion size, percentage of ground-glass opacity areas, and two- and three-dimensional ratios of lesion) assessments in CT images of 72 nodules (25 lung cancers, seven atypical adenomatous hyperplasias, and 40 benign lesions). Optimal criteria specific to benignity were studied.

RESULTS. The prevalence of polygonal shape ($p = 0.005$ and $p = 0.019$, reviewer 1 and reviewer 2), peripheral subpleural lesion ($p = 0.011$ and $p = 0.033$), a predominantly solid lesion ($p < 0.001$ and $p < 0.001$), and three-dimensional ratios ($p < 0.001$ and $p < 0.001$) were greater in benign lesions than in malignancies. The prevalence of a predominantly solid lesion ($p < 0.001$ and $p < 0.001$) was greater in benign lesions than in atypical adenomatous hyperplasias, and the prevalence of a peripheral subpleural lesion ($p = 0.004$ and $p = 0.012$) was greater in atypical adenomatous hyperplasias than in malignancies. Using a single CT feature, polygonal shape and a three-dimensional ratio of greater than 1.78 showed 100% specificity for both reviewers. Among all combinations of CT findings specific to benignity, a combined criterion of a predominantly solid lesion and peripheral subpleural lesion or polygonal shape or the three-dimensional ratio attained the highest sensitivity (63% and 60%) for both reviewers.

CONCLUSION. A combined criterion of CT features was optimal for predicting benign pulmonary lesions.

Since the advent of low-dose helical CT for screening for lung cancer, many small solitary pulmonary nodules (≤1 cm) that were invisible on chest radiographs have been discovered [1, 2]. However, most of the nodules have been benign [1, 2]. In one study, small nodules were detected in 22% of high-risk patients, 90% of whom proved to have benign lesions [2]. On the other hand, primary lung cancer was discovered in 38% of patients who underwent video-assisted thoracic surgery for nodules of 1 cm or smaller detected on CT [3]. Of the 27 lung cancers detected at screening lung CT, 15 (56%) were nodules of 1 cm or smaller [2]. Therefore, how to manage indeterminate small nodules has become a major concern.

As a promising noninvasive procedure, contrast-enhanced CT and positron emission tomography with FDG have been used for differentiating benign from malignant pulmonary nodules [4, 5]. Although Swensen et al. [4] documented 93% accuracy for predicting malignant neoplasms using contrast-enhanced CT, all nodules smaller than 1 cm were excluded from the diagnostic statistics because of technically inadequate CT examinations. Lowe et al. [5] reported 91% accuracy of positron emission tomography for diagnosing malignant lesions. However, all malignant nodules assessed in their series were 1 cm or larger because of limited scanner resolution.

Until now, 2-year stability and benign calcification on radiography or CT have been used for predicting benign nodules [6, 7]. However, the observation policy will burden patients with additional costs, and invasive diagnostic procedures such as CT-guided biopsy or video-assisted thoracoscopy incur patient morbidity. Additionally, the accuracy of CT-guided biopsy is significantly less for small lung nodules (≤15 mm) than for larger

Received December 3, 2001; accepted after revision September 3, 2002.

[1]Department of Radiology, Shinshu University School of Medicine, 3-1-1 Asahi, Matsumoto 390-8621, Japan. Address correspondence to S. Takashima.

[2]Department of Radiology, JA Azumi General Hospital, 3207-1 Ikeda, Nagano 399-8695, Japan.

AJR 2003;180:955–964

0361–803X/03/1804–955

nodules [8], and CT-guided marking before surgery may be required for thoracotomy of small pulmonary nodules because these nodules are often invisible and nonpalpable [9]. Thus, it is clinically useful to establish reliable CT features for benign lesions in small pulmonary nodules. In this study, we retrospectively assessed whether any reliable high-resolution CT features can predict benign lesions in peripheral solitary pulmonary nodules of 1 cm or smaller without benign calcification or fat that are detected at population-based CT screening for lung cancer.

Materials and Methods

During the 3-year period from 1996 through 1998, we conducted a population-based mass screening for lung cancer without charge using a helical CT scanner (CT-W950SR; Hitachi Medical, Tokyo, Japan) loaded in a van [1]. Included in our study were inhabitants in the Nagano prefecture who were 40 years old or older. In this trial, we performed a total of 13,786 CT examinations with low-dose CT scanning with parameters of 25 or 50 mA, 10 mm/sec table speed, an X-ray tube rotation speed of 2 sec, 10-mm collimation, and a pitch of 2. We recommended that all participants receive the initial and two annual repeated screening CT examinations. The number of screened individuals was 5483 in 1996, 4425 in 1997, and 3878 in 1998. Of these, 1259 were examined twice and 3522 were screened three times. Among the total of 13,786 CT scans, 6381 (46%) were conducted in women and 7405 (54%) in men. Regarding smoking habits, 7491 (54%) were nonsmokers and 6295 (46%) were smokers. Among the 6381 women, 5977 (94%) were nonsmokers; among the 7405 men, 1514 (20%) were nonsmokers. Of the 6295 smokers, a history of cigarette smoking was less than 10 pack-years for 4155 (66%), 10–20 pack-years for 1448 (23%), and greater than 20 pack-years for 692 (11%). The median age of the subjects at the initial screening CT was 62 years (age range, 40–74 years).

Two radiologists in consensus interpreted the low-dose CT images displayed on a cathode-ray tube monitor. In reviewing annual repeated CT images, comparison with prior images was performed with side-by-side viewing on a cathode-ray tube monitor with information given about the previous diagnostic CT. We categorized the lesions as follows: unsatisfactory examination (category A), normal (category B), lung abnormality of little clinical importance (category C), noncancerous lung lesion (category D), probable cancer (category E), possible cancer (category Ed), and nodules smaller than 3 mm in diameter (category F). Category D included a solitary pulmonary nodule with benign calcification, a solitary pulmonary nodule that showed no growth on the annual repeated low-dose CT, and lung opacities with segmental distribution. Category E included a solitary pulmonary nodule of 15 mm or larger, a solitary pulmonary nodule with spicular or irregular margins, and a solitary pulmonary nodule that showed interim growth on annual repeated low-dose CT. Category Ed included a solitary pulmonary nodule of 3–14 mm without spicular or irregular margins. Nodules of categories E and Ed had no benign calcification on low-dose CT. We recommended diagnostic CT for individuals with categories E and Ed lesions and annual repeated low-dose CT for individuals with category F lesions. When nodules of category F regressed or remained the same size on annual repeated low-dose CT, they were classified as category D; when the nodules enlarged on the repeated low-dose CT, they were classified as category E. Thus, among the total of 13,786 CT examinations, diagnostic CT, including thin-section high-resolution CT and CT densitometry, was recommended for 477 individuals (3.5%) with categories E or Ed lesions, and annual repeated low-dose CT, for 111 individuals (0.8%) with category F lesions.

Among the 477 individuals (175 of category E and 302 of category Ed), 458 (96%) underwent diagnostic CT. The diagnostic CT was performed within 3 months of screening CT in most individuals. Among these 458 patients, 219 (48%) were diagnosed as having benign lesions because they showed apparent regression (26/219; 12%) or disappearance (152/219; 69%) or had benign calcification (complete, central, laminated, or popcorn calcification; 35/219; 16%) or areas of fat attenuation (–40 to –120 H; 6/219; 3%) on the first diagnostic CT [10, 11]. Among the remaining 239 patients, lung cancer was diagnosed in 73 patients (31%; 61 cases of adenocarcinoma [32 of bronchioloalveolar cell carcinoma, 18 of well-differentiated adenocarcinoma, eight of moderately differentiated adenocarcinoma, and three of poorly differentiated adenocarcinoma], eight of squamous cell carcinoma, and four of small cell carcinoma), atypical adenomatous hyperplasia in nine (4%), and benign lesions in 53 (22%; 10 by surgical resection and 43 by no interim growth for 2 years or more on follow-up diagnostic CT); 94 cases (39%) were thought to be benign on diagnostic CT but had insufficient follow-up with diagnostic CT; and 10 (4%) were lost to follow-up or refused to have surgery.

The 10 patients who were lost to follow-up or refused to have surgery and the 94 patients with lesions thought to be benign were excluded from the 239 cases. Thus, 135 cases remained. Seventy-two cases (53%) were selected from the 135 cases because they had a solitary pulmonary nodule of 1 cm or smaller. According to the latest World Health Organization lung tumor classification, atypical adenomatous hyperplasia is classified as a preinvasive neoplasia of the lung [12]. We treated this neoplasia as an independent entity in this series.

This retrospective study consisted of 25 lung cancers (35%), seven atypical adenomatous hyperplasias (10%), and 40 benign lesions (56%) in 72 cases. The patients were 37 men and 35 women with a mean age of 66 years (age range, 46–75 years). None of the 72 patients had known extrapulmonary malignancy. Nineteen (76%) of the 25 lung cancers were localized bronchioloalveolar carcinoma; the other malignancies were five (20%) adenocarcinoma with bronchioloalveolar carcinoma components and one (4%) squamous cell carcinoma. All atypical adenomatous hyperplasias and eight (20%; nodular fibrosis [n = 4], organizing pneumonia [n = 1], granuloma [n = 1], cryptococcoma [n = 1], and intrapulmonary lymph node [n = 1]) of the 40 benign lesions were surgically resected. The remaining 32 benign lesions (80%) were clinically diagnosed. They were diagnosed as having benign lesions with repeated high-resolution CT performed more than 2 years after the first diagnostic CT because they showed no growth on the follow-up CT scans; 11 lesions decreased in size; three lesions disappeared; and 18 lesions remained the same on the follow-up CT. The time between the first and the follow-up CT was 742–803 days.

All 72 patients underwent diagnostic CT. First, conventional CT scans were obtained through the chest with contiguous 10-mm-thick sections; then helical CT scans were obtained through the lesions using a CT scanner (HiSpeed Advantage; General Electric Medical Systems, Milwaukee, WI) with sequential 1-mm-thick sections during one breath-hold using a pitch of 1. We obtained 10–30 slices per lesion to cover the entire lesion. The images were reconstructed at 0.5-mm intervals with a bone algorithm. Next, three to five coronal multiplanar reformations were acquired at 1-mm intervals through each lesion by one radiologist. The images were photographed using a window level of –550 H and width of 1500 H for lung windows and a level of 35 H and a width of 250 H for mediastinal windows.

First, unaware of the histologic diagnoses, two radiologists independently estimated the likelihood of each lesion being benign or malignant using a 100-point scale based on qualitative assessment of high-resolution CT images. The sensitivity and specificity for predicting benignity were calculated. A score of less than 50 was regarded as indicating benignity.

Next, the same two radiologists independently made qualitative and quantitative evaluations of the high-resolution CT findings. Qualitative evaluation included determination of the presence or absence of lobulation, coarse spiculation, air bronchogram, cavity, satellite lesions, pleural tag, concave margins, polygonal shape, and a peripheral subpleural lesion. Coarse spiculation was defined as the presence of 2-mm or thicker strands extending from the nodule margin into the lung parenchyma without reaching the pleural surface [13]. Satellite lesions were defined as one or more distinctly separate nodular areas of high attenuation located in the same subsegment of the dominant lesion. A pleural tag was defined as a linear strand originating from the nodule surface to reach the pleural surface. Concave margins were defined as a part of the lesion surface (except the portions in contact with the pleura) that showed concave or straightened configuration. Polygonal shape was defined as the entire lesion surface having concave margins only. Interobserver agreement for the nine CT findings was measured using the kappa statistic.

Quantitative evaluation included the measurement of the maximum and minimum diameters of

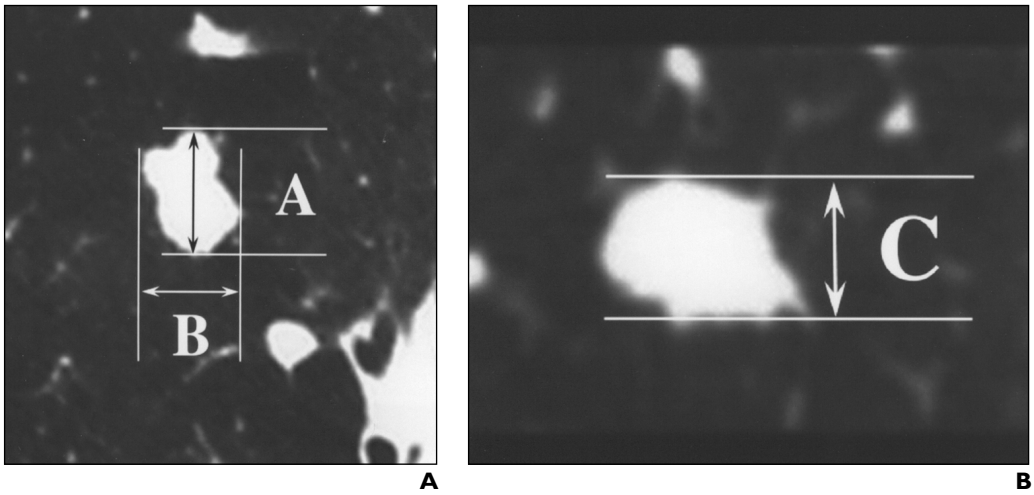

Fig. 1.—Method of measurement in clinically benign lesions.
A, Transverse section in which greatest diameter of lesion was included was selected; diameter was used as maximum transverse diameter (A) of lesion. Minimum transverse diameter (B) of lesion was measured as sum of line segments drawn perpendicular to maximum transverse diameter that reached edges of nodule furthest from line segment corresponding to maximum transverse diameter. Two-dimensional ratio was defined as ratio of A to B.
B, Three to five coronal multiplanar reformations were acquired at 1-mm intervals through each lesion. Longitudinal dimension of lesion was measured as difference between cephalad extent and caudal extent of lesion in each coronal reformation, and greatest value was used as maximum longitudinal dimension (C) of lesion. Three-dimensional ratio was defined as ratio of A to C.

lesions in the transverse plane, the maximum longitudinal dimensions, and the two- and three-dimensional ratios of the lesions. First, the reviewers selected a transverse section in which the greatest diameter of the lesion was included and regarded that diameter as the maximum transverse diameter of the lesion (Fig. 1). The maximum transverse diameter of the lesion was used as a lesion size. Next, the minimum transverse diameter of the lesion was measured as the sum of line segments drawn perpendicular to the maximum transverse diameter that reached the edges of the nodule that were furthest from the line segment corresponding to the maximum transverse diameter. The two-dimensional ratio was defined as the ratio of the maximum to the minimum diameter in the transverse plane. Then the longitudinal dimension of lesion was measured as the difference between the cephalad extent and the caudal extent of the lesion in each coronal reformation; the greatest value was used as the maximum longitudinal dimension of the lesion. The reviewers calculated the ratio of the maximum transverse diameter to the maximum longitudinal dimension of the lesion and used that ratio as a three-dimensional ratio.

The two radiologists also calculated the percentage of ground-glass opacity relative to the entire lesion using the CT images at the level of the greatest transverse diameter of the lesion. To quantify the percentage of ground-glass opacity, we used a dotted grid with equivalent intervals between the horizontal and vertical dots overlaid on the CT images. Without knowledge of the histologic diagnoses, the two reviewers independently counted the number of dots corresponding to the areas of ground-glass opacity and used them as ground-glass opacity areas, and the number of dots corresponding to the lesion was used as an entire lesion. The points on the apparent vessels, normal interlobular septa, and bronchi in the ground-glass opacity areas were counted as ground-glass opacity areas. A cavity in the solid area was regarded as a solid area. We made several overlay grids with different intervals and used an appropriate one so that the number of dots for the entire lesion exceeded at least 30. Then the percentage of ground-glass opacity in the lesion was calculated for each lesion. All the qualitative and quantitative assessments of CT images were performed on the hard-copy images. A predominantly solid lesion was defined as a lesion of ground-glass opacity of less than 50%, and a predominantly ground-glass-opacity lesion was defined as a lesion of ground-glass opacity equal to or greater than 50%. Correlation coefficients of the measurements of the two reviewers were calculated for the lesion size, two- and three-dimensional ratios, and the percentage of

TABLE 1 High-Resolution CT Findings of Reviewer 1

Finding	Benign (n = 40)	Atypical Adenomatous Hyperplasia (n = 7)	Malignant (n = 25)
Lesion size (mm)	7.8 ± 1.7	7.3 ± 0.8	8.3 ± 1.5
Two-dimensional ratio	1.29 ± 0.31	1.21 ± 0.11	1.28 ± 0.28
Three-dimensional ratio	1.62 ± 0.57[a]	1.21 ± 0.21	1.19 ± 0.23[a]
Predominantly solid	36 (90)[a,b]	0[b]	7 (28)[a]
Lobulation	11 (28)	1 (14)	8 (32)
Coarse spiculation	9 (23)	0	3 (12)
Air bronchogram	5 (13)	1 (14)	6 (24)
Cavity	2 (5)	0	1 (4)
Satellite lesion	10 (25)	1 (14)	2 (8)
Pleural tag	12 (30)	0	4 (16)
Concave margin	19 (48)[a]	2 (29)	2 (8)[a]
Polygonal shape	11 (28)[c]	0	0[c]
Peripheral subpleural	12 (30)[d]	4 (57)[e]	1 (4)[d,e]

Note.—Data in first three rows are mean ± SD. Numbers in parentheses are percentages.
[a] $p < 0.001$ between benign and malignant lesions.
[b] $p < 0.001$ between benign and atypical adenomatous hyperplasia lesions.
[c] $p = 0.005$ between benign and malignant lesions.
[d] $p = 0.011$ between benign and malignant lesions.
[e] $p = 0.004$ between atypical adenomatous hyperplasia and malignant lesions.

ground-glass opacity of the lesions to assess interobserver agreement.

We compared all 13 high-resolution CT findings in three lesion categories (benign lesion, atypical adenomatous hyperplasia, and lung cancer). Then we assessed diagnostic statistics for one or every combination of statistically significant CT features and proposed an optimal criterion specific to benignity. One-way analysis of variance followed by the Bonferroni method of multiple comparisons was used to compare the lesion sizes and the two- and three-dimensional ratios of the lesions. The correlation of lesion sizes, ratios of lesions, and the percentages of ground-glass opacity between the two reviewers were examined using Pearson's correlation. Fisher's exact tests were used to compare the prevalence of lobulation, coarse spiculation, predominantly solid lesion, air bronchogram, cavity, satellite lesions, pleural tag, concave margins, polygonal shape, and peripheral subpleural lesion. A p value of less than 0.05 was considered statistically significant. All statistical calculations were performed using statistical software (SPSS, Chicago, IL).

Results

Qualitative Assessment of Thin-Section CT Findings

The kappa value of the two reviewers for the nine qualitative CT features ranged from 0.50 to 0.81. These values indicated moderate to almost perfect agreement [14]. As shown in Tables 1 and 2, a statistically significant difference between benign and malignant lesions (p = 0.005 and p = 0.011, respectively, for reviewer 1; p = 0.019 and p = 0.033, respectively, for reviewer 2) was seen in polygonal shape and peripheral subpleural lesion for both reviewers. The prevalence of polygonal shape (28% vs 0% for reviewer 1; 20% vs 0% for reviewer 2) and peripheral subpleural lesion (30% vs 4% for reviewer 1; 33% vs 8% for reviewer 2) was significantly greater in benign lesions than in malignant lesions for both reviewers. The prevalence of peripheral subpleural lesion (57% vs 4% for reviewer 1; 57% vs 8% for reviewer 2) was significantly greater in atypical adenomatous hyperplasias than in malignant lesions for both reviewers (p = 0.004 for reviewer 1 and p = 0.012 for reviewer 2). The prevalence of concave margin in benign lesions was significantly greater ($p < 0.001$) than that in malignant lesions for reviewer 1, but no significant difference was noted for reviewer 2. The prevalence of these CT findings in each lesion category is summarized in Tables 3 and 4.

TABLE 2 High-Resolution CT Findings of Reviewer 2

Finding	Benign (n = 40)	Atypical Adenomatous Hyperplasia (n = 7)	Malignant (n = 25)
Lesion size (mm)	7.9 ± 1.7	7.0 ± 0.9	8.4 ± 1.5
Two-dimensional ratio	1.28 ± 0.29	1.25 ± 0.19	1.30 ± 0.28
Three-dimensional ratio	1.62 ± 0.56[a]	1.27 ± 0.28	1.18 ± 0.18[a]
Predominantly solid	37 (93)[a,b]	0[b]	5 (20)[a]
Lobulation	9 (23)	1 (14)	5 (20)
Coarse spiculation	8 (20)	0	3 (12)
Air bronchogram	5 (13)	2 (29)	8 (32)
Cavity	1 (3)	0	1 (4)
Satellite lesion	9 (23)	0	2 (8)
Pleural tag	16 (40)	0	5 (20)
Concave margin	17 (43)	2 (29)	4 (16)
Polygonal shape	8 (20)[c]	0	0[c]
Peripheral subpleural	13 (33)[d]	4 (57)[e]	2 (8)[d,e]

Note.—Data in first three rows are mean ± SD. Numbers in parentheses are percentages.

[a] $p < 0.001$ between benign and malignant lesions.

[b] $p < 0.001$ between benign and atypical adenomatous hyperplasia lesions.

[c] p = 0.019 between benign and malignant lesions.

[d] p = 0.033 between benign and malignant lesions.

[e] p = 0.012 between atypical adenomatous hyperplasia and malignant lesions.

Quantitative Assessment of Thin-Section CT Findings

The correlation coefficient was 0.80 for the lesion size ($p < 0.001$), 0.92 for the two-dimensional ratios ($p < 0.001$), 0.94 for the three-dimensional ratios ($p < 0.001$), and 0.94 for the percentage of ground-glass opacity ($p < 0.001$), all of which indicated strong agreement between the two observers' measurements.

A nodule of 3–5 mm and a nodule of 6–10 mm were found in 10 (14%) and 62 (86%) cases, respectively, for reviewer 1, and in nine

TABLE 3 Diagnoses and High-Resolution CT Findings of Reviewer 1

Diagnosis	CT Finding				
	Predominantly Solid	Concave Margin	Polygonal Shape	Peripheral Subpleural	Three-Dimensional Ratio[a]
Malignant (n = 25)					
Localized bronchioloalveolar carcinoma (n = 19)	5	1	0	1	1.22 (0.85–1.78)
Adenocarcinoma with bronchioloalveolar carcinoma pattern (n = 5)	1	1	0	0	1.10 (1.00–1.20)
Squamous cell carcinoma (n = 1)	1	0	0	0	1.00
Atypical adenomatous hyperplasia (n = 7)	0	2	0	4	1.21 (0.83–1.45)
Benign (n = 40)					
Nodular fibrosis (n = 4)	1	4	2	0	1.49 (1.21–2.10)
Organizing pneumonia (n = 1)	1	0	0	0	1.00
Granuloma (n = 1)	1	1	1	0	2.00
Cryptococcoma (n = 1)	1	0	0	0	1.14
Intrapulmonary lymph node (n = 1)	1	0	0	1	2.57
Clinically benign (n = 32)	31	14	8	11	1.63 (0.80–3.20)

[a] Mean (range).

(13%) and 63 (88%) cases, respectively, for reviewer 2. One malignancy (bronchioloalveolar carcinoma) was found among the nodules of 3–5 mm for both reviewers' interpretations. As shown in Tables 1 and 2, a statistically significant difference between benign and malignant lesions was seen for three-dimensional ratios ($p < 0.001$ for both reviewers) and predominantly solid lesions ($p < 0.001$ for both reviewers). The three-dimensional ratio was significantly greater in benign lesions (1.62 ± 0.57 [mean ± SD] for reviewer 1, 1.62 ± 0.56 for reviewer 2) than in malignant lesions (1.19 ± 0.23 for reviewer 1, 1.18 ± 0.18 for reviewer 2). The prevalence of a predominantly solid lesion was significantly greater in benign than in malignant lesions (90% vs 28% for reviewer 1; 93% vs 20% for reviewer 2). The prevalence of a predominantly solid lesion was significantly ($p < 0.001$ for both reviewers) greater in benign lesions than in atypical adenomatous hyperplasias for both reviewers (90% vs 0% for reviewer 1; 93% vs 0% for reviewer 2). The mean values of the three-dimensional ratios of each lesion category are summarized in Tables 3 and 4. The correlation between the numbers of benign, atypical adenomatous hyperplasia,

TABLE 4 Diagnoses and High-Resolution CT Findings of Reviewer 2

Diagnosis	CT Finding				
	Predominantly Solid	Concave Margin	Polygonal Shape	Peripheral Subpleural	Three-Dimensional Ratio[a]
Malignant (*n* = 25)					
Localized bronchioloalveolar carcinoma (*n* = 19)	2	3	0	2	1.21 (0.91–1.64)
Adenocarcinoma with bronchioloalveolar carcinoma pattern (*n* = 5)	2	1	0	0	1.11 (1.00–1.19)
Squamous cell carcinoma (*n* = 1)	1	0	0	0	1.07
Atypical adenomatous hyperplasia (*n* = 7)	0	2	0	4	1.27 (1.00–1.75)
Benign (*n* = 40)					
Nodular fibrosis (*n* = 4)	1	3	2	0	1.42 (1.14–1.90)
Organizing pneumonia (*n* = 1)	1	0	0	0	1.06
Granuloma (*n* = 1)	1	1	1	0	2.00
Cryptococcoma (*n* = 1)	1	0	0	0	1.13
Intrapulmonary lymph node (*n* = 1)	1	0	0	1	2.57
Clinically benign (*n* = 32)	32	13	5	12	1.63 (0.75–3.20)

[a] Mean (range).

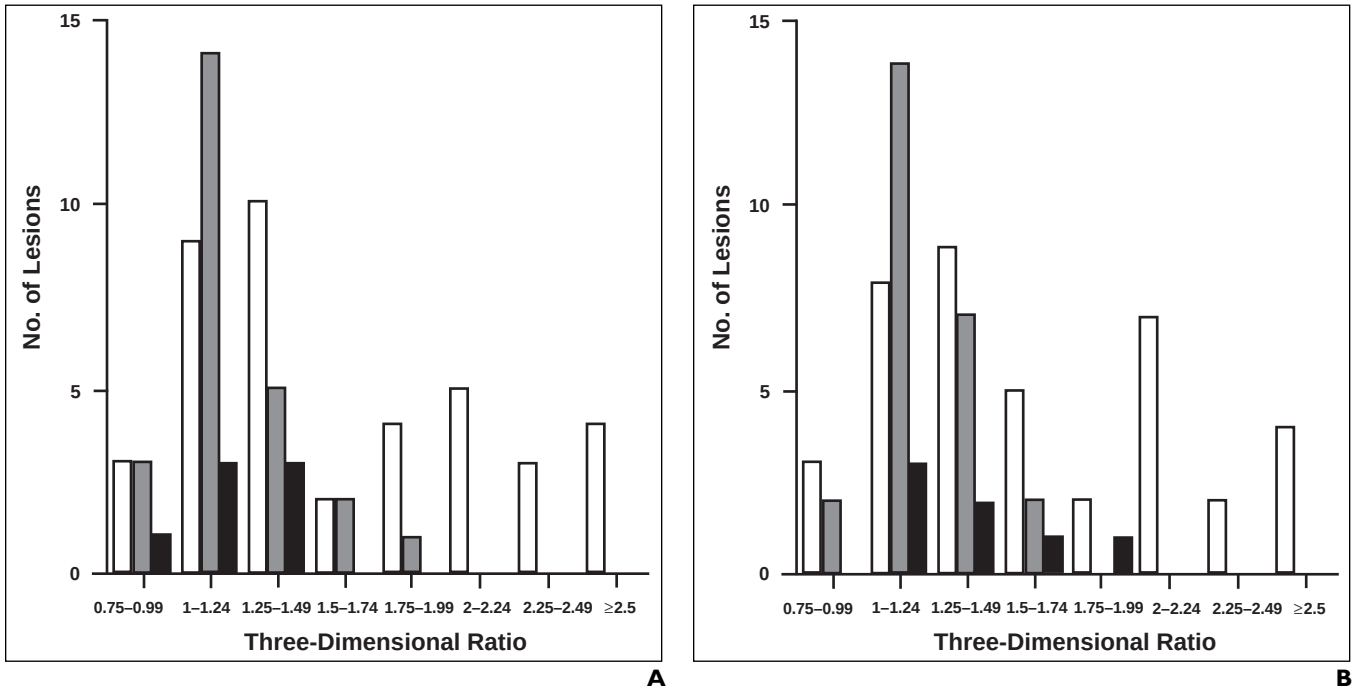

Fig. 2.—Correlation between number of benign (*white*), atypical adenomatous hyperplasia (*black*), and malignant (*gray*) lesions and three-dimensional ratios of lesion.
A and **B,** Bar graphs show correlation between number of benign, atypical adenomatous hyperplasia, and malignant lesions and three-dimensional ratios of lesion for reviewers 1 (**A**) and 2 (**B**). In general, benign lesions had plural peaks, whereas malignant lesions had only one peak in 1.00–1.24. Three-dimensional ratios in malignant lesions did not exceed 1.78.

and malignant lesions and the three-dimensional ratios of the two reviewers is shown in Figure 2. In general, benign lesions had multiple peaks, whereas malignant lesions had only one peak, 1.00–1.24, in the three-dimensional ratios of both reviewers.

Diagnostic Statistics for Predicting Benign Lesions

Diagnostic statistics for differentiating benign lesions from atypical adenomatous hyperplasias and lung cancers in two reviewers are shown in Tables 5 and 6. The sensitivity and specificity for qualitative estimation were 75% and 78%, respectively, for reviewer 1, and 75% and 84%, respectively, for reviewer 2. Seven results were false-positive and 10 were false-negative for reviewer 1; five results were false-positive and 10 were false-negative for reviewer 2.

When we used a single CT feature, the highest accuracy (85% for reviewer 1; 89% for reviewer 2) was obtained with a predominantly solid lesion for both reviewers. However, specificity of the predominantly solid lesion was limited (78% for reviewer 1; 84% for reviewer 2). False-positive results for this predictor were seven for reviewer 1 and five for reviewer 2.

Concave margins had high specificity (88% for reviewer 1; 81% for reviewer 2) for both reviewers, but its sensitivity (48% for reviewer 1; 43% for reviewer 2) was low. As shown in Tables 3 and 4, concave margins were seen in 19 (4/4 with nodular fibrosis, one of one granuloma, and 14/32 clinically benign lesions) of the 40 benign lesions (Fig. 3), two of seven atypical adenomatous hyperplasias, and two (one localized bronchioloalveolar carcinoma and one adenocarcinoma with bronchioloalveolar carcinoma components) of the 25 malignant lesions (Fig. 4) for reviewer 1. This feature was seen in 17 benign lesions (3/4 with nodular fibrosis, 1/1 granuloma, and 13/32 clinically benign lesions), two atypical adenomatous hyperplasias, and four malignant lesions (three localized bronchioloalveolar carcinomas and one adenocarcinoma with bronchioloalveolar carcinoma components) for reviewer 2. On the basis of the meticulous analysis in high-resolution CT images, concave margins were demarcated by the interlobular septa in 18 (78%) of the 23 lesions for reviewer 1 and in 19 (83%) of the 23 lesions for reviewer 2. However, this CT finding was difficult to verify in pathologic studies.

Polygonal shape was specific to benign lesions (100% specificity for both reviewers), but its sensitivity (28% for reviewer 1; 20% for reviewer 2) was low. Eleven benign lesions (two of nodular fibrosis, one granuloma, and eight clinically benign lesions) showed polygonal shape for reviewer 1 (Table 3); eight benign lesions (two of nodular fibrosis, one granuloma, and five clinically benign lesions) showed this feature for re-

TABLE 5 Diagnostic Performance of High-Resolution CT Findings for Predicting Benign Lesions, Reviewer 1

Finding	Sensitivity	Specificity	Accuracy	Positive Predictive Value	Negative Predictive Value
Qualitative estimation	75 (30/40)	78 (25/32)	76 (55/72)	81 (30/37)	71 (25/35)
Concave margin	48 (19/40)	88 (28/32)	65 (47/72)	83 (19/23)	57 (28/49)
Predominantly solid (A)	90 (36/40)	78 (25/32)	85 (61/72)	84 (36/43)	86 (25/29)
Peripheral subpleural (B)	30 (12/40)	84 (27/32)	54 (39/72)	71 (12/17)	49 (27/55)
Polygonal shape (C)	28 (11/40)	100 (32/32)	60 (43/72)	100 (11/11)	52 (32/61)
Three-dimensional ratio > 1.78 (D)	38 (15/40)	100 (32/32)	65 (47/72)	100 (15/15)	56 (32/57)
(A) and (B)	30 (12/40)	100 (32/32)	61 (44/72)	100 (12/12)	53 (32/60)
(C) or (D)	53 (21/40)	100 (32/32)	74 (53/72)	100 (21/21)	63 (32/51)
[(A) and (B)] or (C)	45 (18/40)	100 (32/32)	69 (50/72)	100 (18/18)	59 (32/54)
[(A) and (B)] or (D)	48 (19/40)	100 (32/32)	71 (51/72)	100 (19/19)	60 (32/53)
[(A) and (B)] or (C) or (D)	63 (25/40)	100 (32/32)	79 (57/72)	100 (25/25)	68 (32/47)

Note.—Data are given as percentages. Numbers in parentheses indicate actual numbers of cases.

TABLE 6 Diagnostic Performance of High-Resolution CT Findings for Predicting Benign Lesions, Reviewer 2

Finding	Sensitivity	Specificity	Accuracy	Positive Predictive Value	Negative Predictive Value
Qualitative estimation	75 (30/40)	84 (27/32)	79 (57/72)	86 (30/35)	73 (27/37)
Concave margin	43 (17/40)	81 (26/32)	60 (43/72)	74 (17/23)	53 (26/49)
Predominantly solid (A)	93 (37/40)	84 (27/32)	89 (64/72)	88 (37/42)	90 (27/30)
Peripheral subpleural (B)	33 (13/40)	81 (26/32)	54 (39/72)	68 (13/19)	49 (26/53)
Polygonal shape (C)	20 (8/40)	100 (32/32)	56 (40/72)	100 (8/8)	50 (32/64)
Three-dimensional ratio > 1.78 (D)	38 (15/40)	100 (32/32)	65 (47/72)	100 (15/15)	56 (32/57)
(A) and (B)	33 (13/40)	100 (32/32)	63 (45/72)	100 (13/13)	54 (32/59)
(C) or (D)	50 (20/40)	100 (32/32)	72 (52/72)	100 (20/20)	62 (32/52)
[(A) and (B)] or (C)	43 (17/40)	100 (32/32)	68 (49/72)	100 (17/17)	58 (32/55)
[(A) and (B)] or (D)	50 (20/40)	100 (32/32)	72 (52/72)	100 (20/20)	62 (32/52)
[(A) and (B)] or (C) or (D)	60 (24/40)	100 (32/32)	78 (56/72)	100 (24/24)	67 (32/48)

Note.—Data are given as percentages. Numbers in parentheses indicate actual numbers of cases.

viewer 2 (Table 4). Pathologic studies in one case of nodular fibrosis revealed that the polygonal lesion consisted of dense fibrous tissue with severe contraction (Fig. 5).

Peripheral subpleural lesion had high specificity (84% for reviewer 1; 81% for reviewer 2) for benign lesions, but its sensitivity (30% for reviewer 1; 33% for reviewer 2) was low. Five results were false-positive (one localized bronchioloalveolar carcinoma and four atypical adenomatous hyperplasias) for reviewer 1, and six were false-positive (two localized bronchioloalveolar carcinomas and four atypical adenomatous hyperplasias) for reviewer 2 (Tables 3 and 4).

With respect to the threshold values for three-dimensional ratios, a value greater than 1.78 showed 100% specificity for both reviewers, but its sensitivity (38% for both reviewers) was low. This threshold included the same 15 true-positive cases (one nodular fibrosis, one granuloma, one intrapulmonary lymph node, and 12 clinically benign lesions) for both reviewers. Among the 15 lesions with a value greater than 1.78, a peripheral subpleural lesion was seen in seven lesions (47%) for reviewer 1 and eight lesions (53%) for reviewer 2.

Among the combined criteria of two CT findings, a criterion of a predominantly solid lesion and a peripheral subpleural lesion and a criterion of polygonal shape or a three-dimensional ratio of greater than 1.78 were specific to benign lesions (100% specificity for both reviewers), but the sensitivity (30% and 53%, respectively, for reviewer 1; 33% and 50% for reviewer 2) was still low. A peripheral subpleural lesion with a predominantly solid pattern was seen in 12 benign lesions (one intrapulmonary lymph node and 11 clinically benign lesions) for reviewer 1; of the 12 lesions, seven (58%) had a three-dimensional ratio of greater than 1.78 and 10 (83%) were located in the middle lobe or lower lobe. For reviewer 2, the CT feature of a predominantly solid lesion and a peripheral subpleural lesion was seen in 13 benign lesions (one intrapulmonary lymph node and 12 clinically benign lesions); of the 13 lesions, eight (62%) had a three-dimensional ratio of greater than 1.78 and nine (69%) were located in the middle lobe or lower lobe (Fig. 6).

Among the combined criteria of three or more CT features that had 100% specificity for benign lesions, the highest sensitivity (63% for reviewer 1; 60% for reviewer 2) was attained with the combined criterion of a predominantly solid lesion and a peripheral subpleural lesion or polygonal shape or the three-dimensional threshold value for both reviewers.

Discussion

The prevalence of bronchioloalveolar carcinoma was greater in our trial of screening CT for lung cancer (44% of 73 lung cancers) than in the series (11% of 27 lung cancers) of Henschke et al. [2]. Our trial was performed largely in a group at low risk for lung cancer in rural areas of Japan, whereas the trial of Henschke et al. was carried out in a high-risk group. Only 16% of all participants in our trial were smokers of 10 pack-years or more, whereas all the participants in the series of Henschke et al. were smokers of 10 pack-years or more. Furthermore, 43% of the participants in our series were nonsmoking women. Tobacco smoke is closely related to squamous cell carcinoma and small cell carcinoma but is far less related to bronchioloalveolar carcinoma [15, 16]. Several articles have revealed that the prevalence (20–24% of all lung cancers) of bronchioloalveolar carcinoma, which

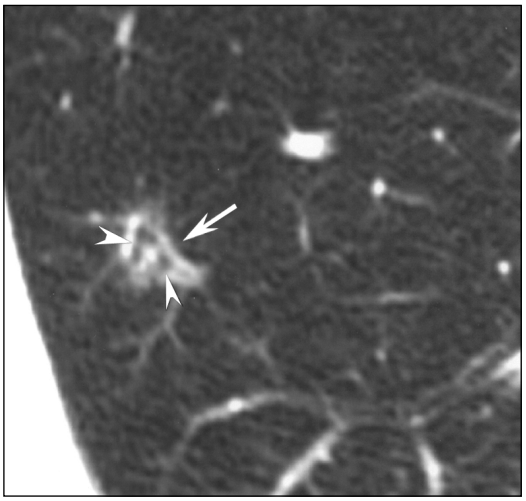

Fig. 3.—Nodular fibrosis with concave margins in 67-year-old man. Both reviewers interpreted lesion as having concave margins (*arrow*), air bronchograms (*arrowheads*), and predominantly ground-glass appearance on transverse high-resolution CT images. Lesion size was measured 8 mm by reviewer 1 and 8.5 mm by reviewer 2. Pathologic diagnosis was nodular fibrosis.

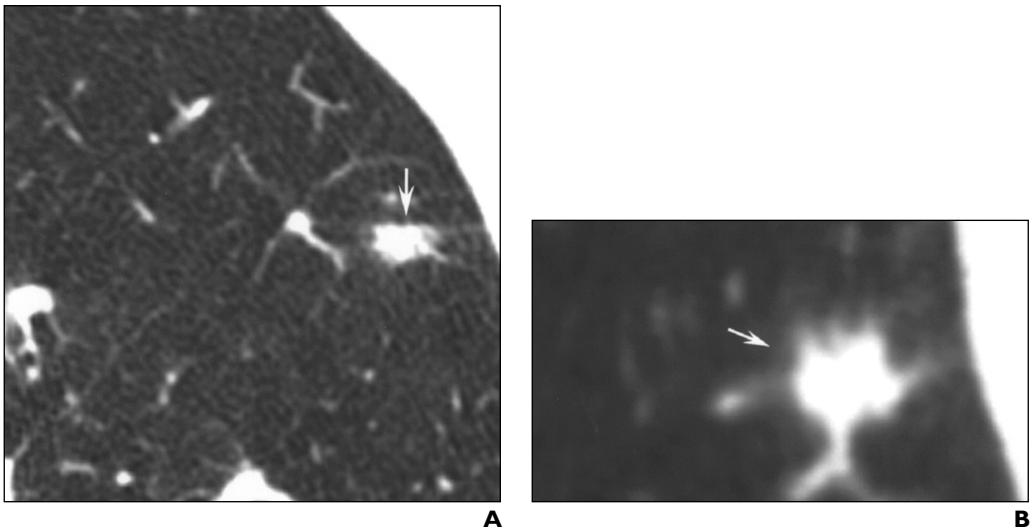

A **B**

Fig. 4.—Localized bronchioloalveolar carcinoma with concave margins in 73-year-old woman.
A, Both reviewers interpreted lesion as having concave margins (*arrow*), being 9 mm, and being predominantly solid on transverse high-resolution CT images. Pathologic diagnosis was localized bronchioloalveolar carcinoma.
B, Coronal reformation shows spherical lesion (*arrow*). Calculated three-dimensional ratio was 1.38 for reviewer 1 and 1.29 for reviewer 2.

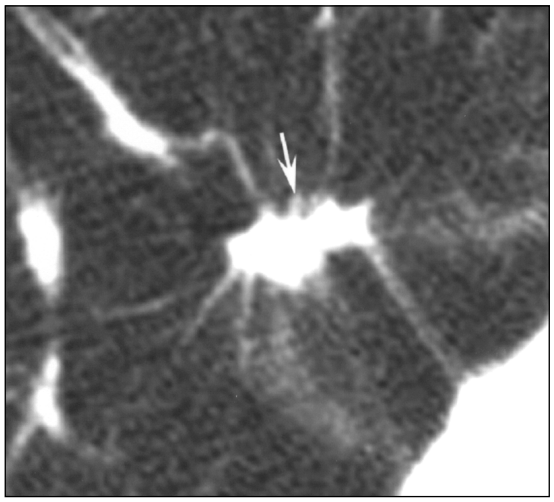

Fig. 5.—Nodular fibrosis with polygonal shape in 72-year-old man. Both reviewers interpreted lesion (*arrow*) as having coarse spiculation, pleural tag, and polygonal shape, and as being predominantly solid on transverse high-resolution CT images. Lesion size was measured as 8 mm by reviewer 1 and 9 mm by reviewer 2. Pathologic diagnosis was nodular fibrosis.

more likely affects nonsmoking women, has dramatically increased in Japan and in other countries in recent years [15, 16]. Sobue et al. [17] reported that the prevalence of squamous cell carcinoma and small cell carcinoma was significantly higher in urban areas (Osaka) than in rural areas (Nagano) in Japan. Thus, we think that the low proportion of heavy smokers, the high proportion of nonsmoking women, the recent increase in the prevalence of bronchioloalveolar carcinoma in women, and the participants in rural areas were the main reasons for the high proportion of bronchioloalveolar carcinoma in our series.

The prevalence of tuberculosis in the Nagano prefecture in which this CT screening for lung cancer was performed was lowest among all prefectures in Japan [18]. The low prevalence of tuberculosis and the low proportion of much cigarette smoking of participants may explain the low frequency (0.8% of all CT examinations) of nodules smaller than 3 mm detected on low-dose CT in this trial.

In this series, we analyzed with CT only solitary pulmonary nodules of 1 cm or smaller for the following reasons: Although most of these pulmonary nodules were benign, more than half of lung cancers detected on screening lung CT belonged to this size category [2]; and although it is hard for contrast-enhanced CT and positron emission tomography with FDG to assess nodules smaller than this size, the diagnosis of nodules of 1 cm or larger can be accurately made with other noninvasive procedures [4, 5]. Swensen et al. [4] reported that malignant lung neoplasms of 1 cm or larger enhanced more than benign lesions on contrast-enhanced CT. Those authors documented 100% sensitivity and 77% specificity for predicting malignancy when they used 20 H in contrast enhancement as a threshold value. Lowe et al. [5] noted 92% sensitivity and 90% specificity for positron emission tomography with FDG for detection of malignant lung nodules of 1 cm or larger that were indeterminate radiographically.

Zwirewich et al. [13] mentioned that greater nodule size and the presence of coarse spiculation, lobulation, and inhomogeneous central CT attenuation were useful high-resolution CT features for predicting malignant lung lesions. However, their study comprised nodules much larger than ours, and these criteria are not applicable to small nodules. Actually, our study has shown very different results: that a predominantly solid lesion, polygonal shape, a peripheral subpleural lesion, and three-dimensional ratios of lesion were statistically significant high-resolution CT features for predicting benignity.

The prevalence of a predominantly solid lesion was significantly greater in benign lesions than in atypical adenomatous hyperplasias or in malignant lesions. According to the literature, most localized bronchioloalveolar carcinomas show a predominantly ground-glass opacity pattern on CT, squamous cell and small cell carcinoma exhibit a predominantly solid pattern, and adenocarcinoma with bronchioloalveolar carcinoma components shows predominantly ground-glass opacity or a solid pattern [19–21]. Most commonly seen benign solitary nodules such as hamartoma or granuloma also show a solid nodule [11, 22]. Other rare benign conditions, including organizing pneumonia, inflammatory pseudotumor, and intrapulmonary lymph node, exhibit a predominantly solid pattern [23–25]. In our study, nodular fibrosis was the main entity among the benign conditions that had a predominantly ground-glass opacity pattern, presumably because ground-glass opacity lesions such as focal infection, hemorrhage, and edema that

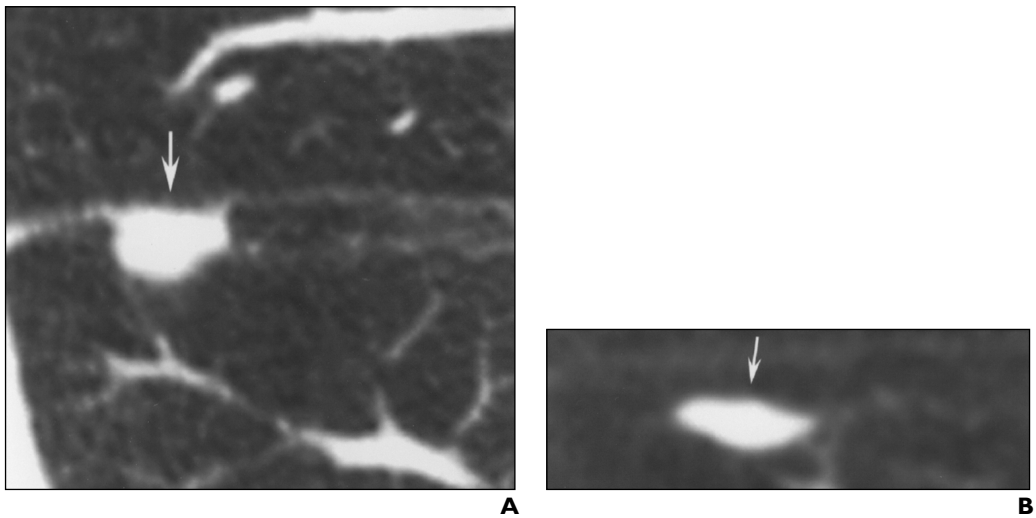

A **B**

Fig. 6.—Intrapulmonary lymph node that showed peripheral subpleural lesion in 53-year-old woman.
A, Both reviewers regarded lesion (*arrow*) as predominantly solid lesion attached to major fissure on transverse high-resolution CT images. Lesion size was measured 9 mm by both reviewers. Pathologic diagnosis was intrapulmonary lymph node.
B, Coronal reformation shows flat lesion (*arrow*). Calculated three-dimensional ratio was 2.57 for both reviewers.

easily change their appearance during a short period of time were already excluded as benign conditions at the first diagnostic CT [26]. As has been reported in the literature, all lesions of atypical adenomatous hyperplasia in our study showed a predominantly ground-glass opacity pattern on CT [27]. Thus, a high proportion of bronchioloalveolar carcinoma in the malignant lesions and the fact that atypical adenomatous hyperplasia was treated as an independent entity may explain why the predominantly solid lesion was a significant factor for benignity in our series.

Polygonal shape was seen solely in benign lesions, but its sensitivity (28% and 20%) was low. All the malignant nodules had at least one or more sides bulging toward the normal lung parenchyma. As verified in the pathologic studies in a case of nodular fibrosis, we think that the polygonal shape represents advanced scar tissue as a result of inflammatory processes of varied causes and that the possibility of malignancy or atypical adenomatous hyperplasia is substantially low.

The three-dimensional ratio was also helpful in predicting benignity; a lesion with the ratio greater than 1.78 invariably indicated benignity for both reviewers. However, its sensitivity (38% for both reviewers) was low. Malignant nodules had a single peak in ratios of 1–1.24 that implied the nodules were spherical; in addition to this peak, benign nodules in general had a second peak in ratios of 2–2.24 that indicated the nodules were flat-shaped in the craniocaudal direction. Neoplastic lesions, regardless of benign or malignant histology, will grow in three-dimensional directions and therefore tend to be spherical, with their three-dimensional ratios reaching 1. About half of the 15 benign lesions with a flat shape were peripheral subpleural lesions, and one of them proved to be an intrapulmonary lymph node. Thus, we think that a flat lesion may represent a benign condition such as an intrapulmonary lymph node, granuloma, or nodular fibrosis.

A peripheral subpleural nodule with predominantly solid attenuation was specific to benign lesions, but its sensitivity (30% and 33%) was low. Most nodules with this CT feature were located in the middle or lower lobe and were flat. A pathologic diagnosis of intrapulmonary lymph node was obtained in one lesion. In the literature, surgically resected intrapulmonary lymph nodes showed well-defined solid masses of less than 15 mm that were located below the carina and within 20 mm of a visceral pleural surface [25]. We consider that most of the peripheral subpleural nodules with predominantly solid attenuation may represent intrapulmonary lymph nodes. Although metastatic tumor, sarcoidosis, pneumoconiosis, and malignant lymphoma should be included in the differential diagnosis for a solid nodule in the perilymphatic areas, all these entities will usually develop multiple lesions often associated with lymphadenopathies in the hilum or mediastinum [28–31]. The absence of extrapulmonary malignancy will considerably reduce the possibility of metastatic tumor. Multiplanar reformations may be helpful in diagnosing peripheral subpleural lesions with predominantly solid attenuation.

Among all criteria that were specific to benign nodules, the highest sensitivities of 63% and 60% were attained with a combined criterion of a peripheral subpleural lesion and a predominantly solid lesion or polygonal shape or the threshold value of greater than 1.78 for three-dimensional ratios. Although the accuracy was almost the same, the criterion was far more specific than the qualitative estimation of the two reviewers (specificities of 78% and 84%). In retrospect, about one third of our 72 cases underwent unnecessary follow-up CT or invasive diagnostic procedures. Thus, our CT criterion may obviate follow-up CT and invasive diagnostic procedures in about three fifths of cases with small benign pulmonary nodules.

Atypical adenomatous hyperplasia was indistinguishable on CT from lung cancer, especially from bronchioloalveolar carcinoma, in our study. Although the number of cases of this entity was small, the only statistical difference was the higher prevalence of a peripheral subpleural location for atypical adenomatous hyperplasia than for lung cancer. Because some authorities advocate the possible conversion of atypical adenomatous hyperplasia to bronchioloalveolar carcinoma, a predominantly ground-glass opacity lesion showing no interim regression should be followed carefully [32].

We acknowledge several limitations in our study. First, we used the traditional criterion of 2-year stability for diagnosing benign lesions. Recently, the 2-year stability rule has come into question because recalculation from the original data revealed that this criterion had only 65% predictive value for benign lesions, and because small changes in size cannot be reliably estimated with chest radiography or CT [7]. Therefore, volumetric analysis rather than diameter has been proposed for assessing the growth rate of small lesions [33]. However, Hasegawa et al. [19] mentioned that solid malignant tumors such as squamous cell carcinoma, small cell carcinoma, or poorly differentiated adenocarcinoma showed rapid growth, with a mean volume doubling time of 149 days. This means that an 8-mm nodule with a doubling time of 149 days can grow to 25 mm over a 2-year period. Almost all lesions (31/32) in which the 2-year stability rule was used were a solid nodule, and lesion size was measured on high-resolution CT images with a pixel size of 0.4 mm in all lesions. Thus, we think that the diagnosis of benign lesion was appropriate for all clinically benign lesions in our series.

Second, this study was biased toward a high proportion of bronchioloalveolar carcinoma. Therefore, our criteria may be valid only for a similar cohort but not for the cohort in a high-risk group. Third, the number of pathologic diagnoses was limited in benign lesions. Fourth, the number of cases in this study was small. Last, our criteria for benignity were determined using mostly the benign nodules that have been documented as not undergoing regression on follow-up CT. Therefore, it would not be appropriate to apply our criteria to pulmonary nodules discovered initially. More work is necessary in a large group of patients with CT–pathologic correlation.

Nonetheless, our study seems to indicate that high-resolution CT analysis is helpful in managing cases with small solitary pulmonary nodules discovered at population-based CT screening for lung cancer. Such analysis may contribute to obviating follow-up CT and invasive diagnostic procedures in patients with small benign nodules in the lung.

References

1. Sone S, Li F, Yang Z-G, et al. Results of three-year mass screening programme for lung cancer using mobile low-dose spiral computed tomography scanner. *Br J Cancer* **2001**;84:25–32
2. Henschke CI, McCauley DI, Yankelevitz DF, et al. Early Lung Cancer Action Project: overall design and findings from baseline screening. *Lancet* **1999**;354:99–105
3. Munden RF, Pugatch R, Liptay MJ, Sugarbaker DJ, Le LU. Small pulmonary lesions detected at CT: clinical importance. *Radiology* **1997**;202:105–110
4. Swensen SJ, Brown LR, Colby TV, Weaver AL. Pulmonary nodules: CT evaluation of enhancement with iodinated contrast material. *Radiology* **1995**;194:393–398
5. Lowe VJ, Fletcher JW, Lawson M, et al. Prospective investigation of positron emission tomography in lung nodules. *J Clin Oncol* **1998**;16:1075–1084
6. Webb WR. Radiologic evaluation of the solitary pulmonary nodule. *AJR* **1990**;154:701–708
7. Yankelevitz DF, Henschke CI. Does 2-year stability imply that pulmonary nodules are benign? *AJR* **1997**;168:325–328

8. Li H, Boiselle PM, Shepard JO, Trotman-Dickenson B, McLoud TC. Diagnostic accuracy and safety of CT-guided percutaneous needle aspiration biopsy of the lung: comparison of small and large pulmonary nodules. *AJR* **1996**;167:105–109
9. Tsuchida M, Yamato Y, Aoki T, et al. CT-guided agar marking for localization of nonpalpable peripheral pulmonary lesions. *Chest* **1999**;116:139–143
10. Siegelman SS, Khouri NF, Leo FP, Fishman EK, Braverman RM, Zerhouni EA. Solitary pulmonary nodules: CT assessment. *Radiology* **1986**; 160:307–312
11. Siegelman SS, Khouri NF, Scott WW Jr, et al. Pulmonary hamartoma: CT findings. *Radiology* **1986**;160:313–317
12. Travis WD, Colby TV, Corrin B, et al. *International histological classification of tumors: histopathologic typing of lung and pleural tumors*, 3rd ed. Geneva: World Health Organization, **1999**
13. Zwirewich CV, Vedal S, Miller RR, Müller NL. Solitary pulmonary nodule: high-resolution CT and radiologic–pathologic correlation. *Radiology* **1991**;179:469–476
14. Sackett DL, Haynes RB, Guyatt GH, Tugwell P. The clinical examination. In: Sackett DL, Haynes RB, Guyatt GH, Tugwell P, eds. *Clinical epidemiology: a basic science for clinical medicine*, 2nd ed. Boston: Little, Brown, **1991**:19–49
15. Auerbach O, Garfinkel L. The changing pattern of lung carcinoma. *Cancer* **1991**;68:1973–1977
16. Barsky SH, Cameron R, Osann KE, Tomita D, Holmes EC. Rising incidence of bronchioloalveolar lung carcinoma and its unique clinicopathologic features. *Cancer* **1994**;73:1163–1170
17. Sobue T, Tsukuma H, Oshima A, et al. Lung cancer incidence rates by histologic type in high- and low-risk areas; a population-based study in Osaka, Okinawa, and Saku Nagano, Japan. *J Epidemiol* **1999**;9:134–142
18. Annual Reports of Surveillance of Tuberculosis in 2000 of Japan, The Ministry of Health, Labour, and Welfare of Japan. Available at http://www.mhlw.go.jp/index.html. Accessed July **2002**
19. Hasegawa M, Sone S, Takashima S, et al. Growth rate of small lung cancers detected on mass CT screening. *Br J Radiol* **2000**;73:1252–1259
20. Yabuuchi H, Murayama S, Sakai S, et al. Resected peripheral small cell carcinoma of the lung: computed tomographic-histologic correlation. *J Thorac Imaging* **1999**;14:105–108
21. Yang Z-G, Sone S, Takashima S, et al. High-resolution CT analysis of small peripheral lung adenocarcinomas revealed on screening helical CT. *AJR* **2001**;176:1399–1407
22. Lee JY, Lee KS, Jung KJ, et al. Pulmonary tuberculosis: CT and pathologic correlation. *J Comput Assist Tomogr* **2000**;24:691–698
23. Kohno N, Ikezoe J, Johkoh T, et al. Focal organizing pneumonia: CT appearance. *Radiology* **1993**; 189:119–123
24. Agrons GA, Rosado-de-Christenson ML, Kirejczyk WM, Conran RM, Stocker JT. Pulmonary inflammatory pseudotumor: radiologic features. *Radiology* **1998**;206:511–518
25. Matsuki M, Noma S, Kuroda Y, Oida K, Shindo T, Kobashi Y. Thin-section CT features of intrapulmonary lymph nodes. *J Comput Assist Tomogr* **2001**;25:753–756
26. Collins J, Stern EJ. Ground-glass opacity at CT: the ABCs. *AJR* **1997**;169:355–367
27. Kushihashi T, Munechika H, Ri K, et al. Bronchioloalveolar adenoma of the lung: CT–pathologic correlation. *Radiology* **1994**;193:789–793
28. Murata K, Takahashi M, Mori M, et al. Pulmonary metastatic nodules: CT–pathologic correlation. *Radiology* **1992**;182:331–335
29. Müller NL, Kullnig P, Miller RR. The CT findings of pulmonary sarcoidosis: analysis of 25 patients. *AJR* **1989**;152:1179–1182
30. Remy-Jardin M, Beuscart R, Sault MC, Marquette CH, Remy J. Subpleural micronodules in diffuse infiltrative lung diseases: evaluation with thin-section CT scans. *Radiology* **1990**;177:133–139
31. Lewis ER, Caskey CI, Fishman EK. Lymphoma of the lung: CT findings in 31 patients. *AJR* **1991**;156:711–714
32. Kitamura H, Kameda Y, Nakamura N, et al. Atypical adenomatous hyperplasia and bronchoalveolar lung carcinoma: analysis by morphometry and the expression of p53 and carcinoembryonic antigen. *Am J Surg Pathol* **1996**;20:553–562
33. Yankelevitz DF, Reeves AP, Kostis WJ, Zhao B, Henschke CI. Determination of malignancy in small pulmonary nodules based on volumetrically determined growth rate. (abstr) *Radiology* **1998**;209(P):375